HHS Public Access

Author manuscript

Abdom Radiol (NY). Author manuscript; available in PMC 2022 January 02.

Published in final edited form as:

Abdom Radiol (NY). 2021 December ; 46(12): 5772–5780. doi:10.1007/s00261-021-03234-1.

Diagnostic abdominal MR imaging on a prototype low-field 0.55 T scanner operating at two different gradient strengths

Hersh Chandarana[1], **Barun Bagga**[1], **Chenchan Huang**[1], **Bari Dane**[1], **Robert Petrocelli**[1], **Mary Bruno**[1], **Mahesh Keerthivasan**[2], **David Grodzki**[3], **Kai Tobias Block**[1], **David Stoffel**[1], **Daniel K. Sodickson**[1]

[1]Department of Radiology, Center for Advanced Imaging Innovation and Research (CAI2R), New York University Grossman School of Medicine, 660 First Ave, New York, NY 10016, USA

[2]Siemens Medical Solutions USA Inc., Malvern, PA, USA

[3]Siemens Healthcare GmbH, Erlangen, Germany

Abstract

Purpose—To develop a protocol for abdominal imaging on a prototype 0.55 T scanner and to benchmark the image quality against conventional 1.5 T exam.

Methods—In this prospective IRB-approved HIPAA-compliant study, 10 healthy volunteers were recruited and imaged. A commercial MRI system was modified to operate at 0.55 T (LF) with two different gradient performance levels. Each subject underwent non-contrast abdominal examinations on the 0.55 T scanner utilizing higher gradients (LF-High), lower adjusted gradients (LF-Adjusted), and a conventional 1.5 T scanner. The following pulse sequences were optimized: fat-saturated T2-weighted imaging (T2WI), diffusion-weighted imaging (DWI), and Dixon T1-weighted imaging (T1WI). Three readers independently evaluated image quality in a blinded fashion on a 5-point Likert scale, with a score of 1 being non-diagnostic and 5 being excellent. An exact paired sample Wilcoxon signed-rank test was used to compare the image quality.

Results—Diagnostic image quality (overall image quality score ≥ 3) was achieved at LF in all subjects for T2WI, DWI, and T1WI with no more than one unit lower score than 1.5 T. The mean difference in overall image quality score was not significantly different between LF-High and LF-Adjusted for T2WI (95% CI − 0.44 to 0.44; $p = 0.98$), DWI (95% CI − 0.43 to 0.36; $p = 0.92$), and for T1 in- and out-of-phase imaging (95%C I − 0.36 to 0.27; $p = 0.91$) or T1 fat-sat (water only) images (95% CI − 0.24 to 0.18; $p = 1.0$).

✉Hersh Chandarana, Hersh.Chandarana@nyulangone.org.

Author contributions All authors have fulfilled ICJME criteria for authorship.

Supplementary Information The online version contains supplementary material available at https://doi.org/10.1007/s00261-021-03234-1.

Consent to Participate Yes.

Ethical Approval IRB approved prospective study.

Conclusion—Diagnostic abdominal MRI can be performed on a prototype 0.55 T scanner, either with conventional or with reduced gradient performance, within an acquisition time of 10 min or less.

Keywords

Low-field MRI; Abdominal MRI; Accessible MRI; Low-cost MRI

Introduction

The majority of clinical MRI scanners today operate with field strengths ranging from 1.5 to 3 T. MRI of the abdomen at these field strengths is usually performed as a “problem-solving tool” rather than a first-line diagnostic examination due to its high cost and limited accessibility. To overcome cost barriers and accessibility limitations for MRI various groups have proposed abbreviated examination protocols, in which certain sequences that are deemed less important are eliminated [1, 2]. However, there is no consensus about which sequences to eliminate or about the impact of the abbreviated protocol either on diagnostic accuracy or on recall rate due to exams with limited diagnostic value. Another approach is to utilize novel methods for accelerating MR sequences by reconstructing images from undersampled acquisitions using techniques like compressed sensing and machine learning [3, 4]. Although these two approaches have shown considerable promise, a complementary approach would be to rethink the cost and accessibility of the imaging hardware, i.e., the MR scanner itself.

Two subcomponents of the scanner hardware, the magnet and the gradient infrastructure, account for over 50% of the overall cost of a typical 1.5 T system. Current attention to the MR value proposition [5] coupled with recent advances in image acquisition and reconstruction techniques has reignited interest in imaging at lower field strength (≤ 1 T) [6]. Such lower-field scanners not only decrease the cost of the magnet but also lower the siting cost. Head-only scanners with 0.5 T and with 0.064 T field strength have been recently approved by the FDA, highlighting the potential of scanning at lower field strengths [7, 8]. Feasibility of functional cardiac imaging has also been demonstrated at a lower field strength of 0.35 T [9]. Furthermore, a prototype 0.55 T whole-body scanner has been recently investigated for cardiopulmonary imaging [10–12]. In addition to the magnet, another major contributor to the overall cost of the MR system is the gradient system and associated power and cooling requirements. Systems operating with low field and relaxed gradient specifications not only lower the initial capital cost but also decrease total cost of ownership (TCO) due to lower footprint and decreased power and cooling needs. Such a combination is expected to achieve 40 to 50% reduction in scanner cost as well as total cost of ownership.

Therefore, the purpose of this study was to investigate if a high-performance, low-field strength 0.55 T MRI system operating with two different gradient strengths can generate MR images of the abdomen with diagnostic image quality and to benchmark the image quality by comparing it to the image quality achieved with a conventional 1.5 T scanner.

Materials and methods

Two of the authors are employees of Siemens Healthcare/Healthineers. Under an existing research agreement, these authors provided technical support with the modification of the MRI system and with sequence modifications for operation at 0.55 T. These authors did not have control over any other aspect of the study design or the study results.

Subjects

In this prospective IRB-approved HIPAA-compliant study, 10 healthy volunteers (4F, 6M; mean age 33.1 years, range 26–42 years) were recruited to undergo three separate MRI examinations for research purposes between March 1, 2020 and October 31, 2020. Informed consent was obtained from all the subjects before the imaging sessions.

MRI scanner

A commercial MRI system (MAGNETOM Aera 1.5 T, Siemens Healthcare, Erlangen, Germany) was modified to operate as a prototype scanner at a field strength of 0.55 T. The modified scanner provides two different gradient performance levels (higher/conventional: maximum gradient amplitude 45 mT/m, maximum slew rate 200 T/m/s; lower/adjusted: maximum gradient amplitude 25 mT/m, maximum slew rate 40 T/m/s). A 6-channel body array and 18-channel spine array were tuned to 0.55 T field strength and used for imaging. Each subject underwent three MR examinations of the abdomen with imaging performed on (1) the prototype 0.55 T scanner utilizing higher-performance gradients (LF-High), (2) the prototype 0.55 T with lower-performance gradients (LF-Adjusted), and (3) a conventional 1.5 T scanner with high-performance gradients (MAGNETOM Sola, Siemens Healthcare, Erlangen Germany; maximum gradient amplitude 45 mT/m, maximum slew rate 200 T/m/s).

Sequence details

Our routine abdominal MRI protocol includes axial fat-saturated T2-weighted imaging (T2WI), axial diffusion-weighted imaging (DWI), and axial Dixon T1-weighted imaging (T1WI, including T1 in- and out-of-phase and water only or T1W fat-saturated). Routine liver/abdominal MR imaging also includes T1W fat-saturated post-contrast imaging at multiple time points after contrast injection. For this research study, we did not administer intravenous contrast. Hence, post-contrast T1W (or water only) images were not acquired. However, a Dixon T1W acquisition could easily be appended to our study protocol to perform post-contrast imaging. Non-contrast sequences were optimized on the LF scanner as follows (Table 1):

1. T2WI was performed with a fat-suppressed free-breathing turbo-spin-echo sequence using a BLADE trajectory [13] instead of conventional Cartesian scanning. Oversampling in the k-space center of the BLADE trajectory allowed for correction of bulk motion and permitted non-triggered free-breathing imaging. A BLADE coverage factor of 121% was used to improve SNR and to reduce artifacts. The lower specific absorption rate (SAR) at 0.55 T permitted the use of 180° flip angles for the refocusing pulses. Furthermore, to improve the fat-suppression performance at 0.55 T, an asymmetric, adiabatic full-passage-

skewed Spectral Adiabatic Inversion Recovery (SPAIR) RF pulse with inversion times optimized for the low field strength was used to suppress multi-spectral fat signal [14].

2. Axial DWI was performed using an echo-planar imaging (EPI) sequence at three *b* values (50, 500, 800 s/mm^2). For each *b* value, data were acquired in three orthogonal diffusion gradient directions which were combined to generate the trace diffusion-weighted images used to reconstruct an ADC map. Since the minimum TE in an EPI sequence is controlled by the number of readouts per shot, parallel imaging (acceleration factor = 2) and partial Fourier sampling were used to maintain clinically acceptable echo times. To overcome the lower SNR at 0.55 T, more averages were acquired for each *b* value (see Table 1). As EPI sequences are strongly dependent on the gradient performance (gradient slew rate and amplitude), the effective TE was longer with the lower-performance adjusted gradient system.

3. Axial Dixon T1WI images were acquired in a breath-hold by optimizing a conventional T1-weighted Dixon 3D GRE sequence. Readouts at two TEs were acquired to separate the fat and water components. The fat/water resonance frequency difference decreases at lower field strength: the frequency difference for the dominant fat peak is approximately 220 Hz at 1.5 T and only 80 Hz at 0.55Tm, resulting in longer in-phase and out-of-phase echo times at lower fields (TE_op = 2.2 ms, TE_in = 4.5 ms at 1.5 T and TE_op = 6.2 ms, TE_in = 12.5 ms at 0.55 T). Using a conventional two-point Dixon acquisition that samples these longer TE times would result in a 30-s scan (which is not acceptable for a breath-hold acquisition). To reduce the overall measurement time, data were acquired at two arbitrary TEs of 2.5 ms and 6 ms, and a flexible echo time Dixon algorithm [15] was used to reconstruct the fat and water T1W images. The longer TR of 9 ms required use of parallel imaging with fourfold acceleration to keep the scan time within a 16-s breath-hold.

Details of the acquisition parameters for the above-mentioned sequences are listed in Table 1.

Assessment of image quality

Two board-certified fellowship-trained radiologists and one abdominal imaging fellow independently evaluated the image quality of axial fat-sat T2WI, axial DWI, axial T1WI in- and out-of-phase, and axial T1FS data sets acquired at low field with high gradients, at low field with adjusted gradients, and at 1.5 T with conventional high gradients. These datasets were randomly presented to the readers who were blinded to the imaging hardware and acquisition parameters. The readers evaluated parameters of image quality on a 5-point Likert scale, with a score of 1 indicating non-diagnostic and a score of 5 indicating excellent image quality (Table 2).

Assessment of liver-to-muscle contrast ratio

Quantitative assessment of liver-to-muscle contrast ratio was performed by a reader blinded to the acquisition scheme. Analysis was performed for T2WI, DWI (high *b* value acquisition), and T1FS image contrasts. Reader placed two regions of interest (ROI) on a single axial slice in the liver parenchyma, in the right and left lobe, respectively, at the level of the main portal vein and on the slice above and below this level. Hence, a total of 6 ROIs on three consecutive axial slices in the liver parenchyma per patient were sampled and averaged to get liver signal intensity (Lc). At the same level ROIs were also placed on the paraspinal right and left muscle for 2 ROIs per slice and a total of 6 ROIs over 3 slices. These muscle ROIs were averaged to obtain average muscle signal intensity (Mc). Liver-to-muscle contrast ratio (Lc/Mc) was computed for each subject for all three acquisitions.

Statistical analysis

An exact paired sample Wilcoxon signed-rank test was used to compare the imaging hardware (denoted LF-High, LF-Adjusted, 1.5 T) in terms of the 5-point ordinal scores for each aspect of image quality. The comparisons were first stratified by image contrast and reader and then stratified by image contrast with the scores for each subject represented as an average over readers. The mean within-subject difference between the three types of hardware is compared in terms of the 5-point ordinal scores for each aspect of image quality for each image contrast. The exact significance level (p) from the pairwise comparison of image contrasts for the three hardware types resulting from the application of a Wilcoxon signed-rank test to the within-subject difference between acquisitions in terms of the image quality scores for each image contrast was computed.

Inter-reader agreement was assessed in terms of the linear weighted kappa coefficient and the percentage of times two readers provided concordant results for the same image. The level of agreement was interpreted as poor when kappa (K) was less than zero, slight when $0 \leq K \leq 0.2$, fair when $0.2 < K \leq 0.4$, moderate when $0.4 < K \leq 0.6$, substantial when $0.6 < K \leq 0.8$, and almost perfect when $K > 0.8$. The statistical tests were conducted at the two-sided 5% significance level using SAS 9.4 software (SAS Institute, Cary, NC).

Lc/Mc ratio was compared between LF-High, LF-Adjusted, and 1.5 T for T2WI, DWI, and T1FS image contrasts using paired sample *t* test with two-tailed 5% significance level. This analysis was performed using MedCalc® Statistical Software version 19.8 (MedCalc Software Ltd, Ostend, Belgium; https://www.medcalc.org; 2021).

Results

For each examination, as mentioned above the following image contrasts were acquired: axial fat-sat T2WI, axial DWI, axial breath-hold T1 Dixon with T1 in- and out-of-phase, and T1FS. A total of 120 acquisitions (30 exams and 4 image contrasts each) were independently assessed by three radiologists in a blinded fashion.

T2WI

Overall image quality scores for T2WI averaged over three readers and stratified by each reader are shown in Table 3. Other parameters of image quality are shown in the Supplement Table S1. The overall image quality score for LF-High was 4.1 ± 0.6, for LF-Adjusted it was 4.1 ± 0.6, and for 1.5 T it was 4.6 ± 0.4. The mean difference in overall image quality score was not significantly different between LF-High and LF-Adjusted (95% CI − 0.44 to 0.44; $p = 0.98$) or between 1.5 T and LF-High (95% CI − 0.06 to 1.06; $p = 0.09$). However, the mean difference in image quality score between 1.5 T and LF-Adjusted was significant (95% CI 0.16 to 0.84; $p = 0.016$).

In 9 out of 10 cases (90%), the overall image quality on LF-High and LF-Adjusted was no more than one unit lower than the corresponding rating on the 1.5 T scanner. When averaged over three readers, each subject had an image quality score ≥ 3 on LF-High and LF-Adjusted acquisition (Fig. 1).

DWI

Overall image quality scores for DWI averaged over three readers and stratified by each reader are shown in Table 3. Other parameters of image quality are shown in the Supplement Table S2. The overall image quality score for LF-High was 4.1 ± 0.5, for LF-Adjusted was 4.1 ± 0.5, and for 1.5 T was 4.6 ± 0.3. The mean difference in overall image quality score was not significantly different between LF-High and LF-Adjusted (95% CI − 0.43 to 0.36; $p = 0.92$) or between 1.5 T and LF-High (95% CI − 0.06 to 1.0; $p = 0.125$). However, the mean difference in image quality score between 1.5 T and LF-Adjusted was significant (95% CI 0.08 to 0.79; $p = 0.01$).

In 9 out of 10 cases (90%), the DWI overall image quality on LF-High was no more than one unit lower than the corresponding rating for the 1.5 T scanner and in 8 out of 10 cases (80%) the overall image quality on LF-Adjusted was no more than one unit lower than the corresponding rating on 1.5 T scanner. When averaged over three readers, each subject had an image quality score ≥ 3 on LF-High and LF-Adjusted acquisitions (Fig. 2).

T1WI in- and out-of-phase

Overall image quality scores for T1WI in- and out-of-phase averaged over the three readers and stratified by each reader are shown in Table 3. Other parameters of image quality are shown in the Supplement Table S3. The overall image quality score for LF-High was 4.5 ± 0.4, for LF-Adjusted was 4.4 ± 0.3, and for 1.5 T was 4.9 ± 0.1. The mean difference in overall image quality score was not significantly different between LF-High and LF-Adjusted (95% CI − 0.36 to 0.27; $p = 0.91$). The mean difference in overall image quality score was significantly higher at 1.5 T when compared to LF-High (95% CI 0.2 to 0.8; $p = 0.03$) and LF-Adjusted (95% CI 0.27 to 0.73; $p = 0.004$). However, it is important to note that in 100% of the cases, the overall image quality scores on LF-High and LF-Adjusted were no more than one unit lower than the corresponding ratings on the 1.5 T exam. When averaged over three readers, each subject had an image quality score ≥ 3 on LF-High and LF-Adjusted.

Fat-sat T1WI

Overall image quality scores for axial fat-sat T1WI averaged over three readers and stratified by each reader are shown in Table 3. Other parameters of image quality are shown in the Supplement Table S4. The overall image quality score for LF-High was 4.3 ± 0.3, for LF-Adjusted it was 4.27 ± 0.2, and for 1.5 T it was 4.97 ± 0.1. The mean difference in overall image quality score was not significantly different between LF-High and LF-Adjusted (95% CI − 0.24 to 0.18; $p = 1.0$). The mean overall image quality score averaged over the three readers was significantly higher for 1.5 T when compared to LF-High (95% CI 0.47 to 0.86; $p = 0.004$) as well as LF-Adjusted (95% CI 0.56 to 0.84; $p = 0.002$). However, it is important to note that in 100% of cases, the overall image quality scores on LF-High and LF-Adjusted were no more than one unit lower than the corresponding rating on the 1.5 T exam. When averaged over three readers, each subject had an image quality score ≥ 3 on LF-High and LF-Adjusted (Fig. 3).

Inter-reader agreement

The percentage (fraction) of times two readers provided concordant results for overall image quality when assessing the same image was 55.2% with linear weighted kappa coefficient of 0.242.

Liver-to-muscle contrast ratio

Liver-to-muscle contrast signal intensity ratios (Lc/Mc) for T2WI, DWI, and T1FS are as shown in Table 4.

T2WI: The difference in Lc/Mc between LF-High and LF-Adjusted did not reach statistical significance ($p = 0.055$). However, Lc/Mc at 1.5 T was significantly higher than at LF-High and LF-Adjusted ($p < 0.001$).

DWI: LF-High and LF-Adjusted had significantly higher Lc/Mc when compared to 1.5 T ($p < 0.001$). Furthermore, LF-Adjusted had higher Lc/Mc when compared to LF-High ($p = 0.01$).

T1FS: LF-High and LF-Adjusted had significantly higher Lc/Mc when compared to 1.5 T ($p < 0.001$). Furthermore, LF-High had higher Lc/Mc when compared to LF-Adjusted but this did not reach statistical significance ($p = 0.07$).

Discussion

Our initial experience demonstrates that, for imaging performed with LF-High and LF-Adjusted configurations, T2WI, DWI, and T1WI in all ten subjects received overall image quality score of ≥ 3 when averaged over three readers, consistent with diagnostic or better overall image quality. Hence, conventional sequences can be modified to provide diagnostic abdominal imaging on a 0.55 T scanner with regular strength gradients as well as with lower-performance adjusted gradients within an acquisition time that is clinically acceptable (non-contrast sequences with a total scan time of less than 10 min).

MRI has limited accessibility worldwide due to the high cost of the scanner as well as associated sitting costs and power requirements (initial capital cost and TCO). To achieve

the value proposition of MRI as a first-line imaging modality for various applications such as oncologic imaging, the MRI exam and the scanner need to be cheaper and have a lower TCO. To address this need and investigate various potential solutions, we have recently installed a new prototype scanner operating at a lower field strength (0.55 T) in a dedicated test bay at our institution. Unlike traditional low-field systems, the scanner features two sets of gradients (higher/regular and lower/adjusted) and state-of-the-art programming capabilities. Such a scanner design incorporating a lower field magnet and gradients with adjusted performance can potentially achieve 40 to 50% reduction in the hardware cost as well as TCO when compared to a conventional 1.5 T scanner, which could translate into lower examination cost. These benefits would result from (1) a cheaper magnet, RF amplifier and gradient system, (2) decreased siting cost due to a lighter weight and smaller footprint, and (3) decreased power and cooling requirements. In addition, a lower field strength may potentially improve robustness due to decreased susceptibility and artifacts and improved patient compliance due to lower acoustic noise and reduced vestibular upset. Recently a low-field scanner operating at 0.55 T received an FDA approval. Such a scanner is expected to have lower capital and operation costs and would be easier to site and thus may provide an opportunity to image patients that may otherwise be difficult to image.

The purpose of our study was to test if diagnostic imaging can be performed reliably on such a system. We performed T2WI on the LF scanner with a free-breathing BLADE acquisition in 3 min and 14 s, which was longer than the acquisition time of approximately 1 min and 19 s on the conventional 1.5 T scanner. To maintain the acquisition time, of approximately 3 min, we increased the slice thickness from 4 to 6 mm on LF while maintaining in-plane resolution. Overall image quality scores on the 1.5 T scanner were higher compared to LF. However, all LF images were scored as diagnostic irrespective of the gradient strength (score ≥ 3). Similar to T2WI, the overall image quality of free-breathing DWI on LF was not significantly different between LF-High and LF-Adjusted, and it was scored as diagnostic (or better) for all subjects. DWI was performed within an acquisition time of 5 min and 9 s. T1W Dixon imaging was performed in a 16-s breath-hold acquisition on LF. As the in- and out-of-phase echo times are much longer at lower field, this was only possible with the use of a parallel-imaging factor of 4. The overall image quality was not significantly different between LF-High and LF-Adjusted for in- and out-of-phase, as well as for T1FS. It is important to note that in all cases, images were diagnostic and no more than one unit lower than at 1.5 T.

Imaging at low field strength requires a balance between acquisition time, image quality, and resolution. In this study, our goal was to modify conventional sequences so that abdominal imaging can be performed on a LF scanner at two different gradient strengths. In order to maintain a clinically acceptable acquisition time of 10 min or less for the non-contrast component of the abdominal exams, we modified various sequence parameters and reduced the slice resolution. However, these changes are still within the expected range for liver/abdominal MRI protocols (as per ACR practice guidelines).

As a next step, there is a need to perform a head-to-head comparison between LF and 1.5 T imaging hardware for lesion detection and characterization. Furthermore, there is a need to modify the conventional acquisition and reconstruction schemes to take advantage of the

longer T2* at LF and to utilize advances in compressed sensing and machine learning to reconstruct diagnostic images from highly undersampled data [3, 4, 16].

In conclusion, this study showed that using a prototype scanner operating at 0.55 T is feasible for diagnostic abdominal imaging at 0.55 T within an examination time that is clinically acceptable. Clinical implementation of such low-field scanners will decrease the hardware cost as well as siting cost, hence lowering the capital and overall cost of MRI exams and potentially improving accessibility of MRI for abdominal imaging.

Supplementary Material

Refer to Web version on PubMed Central for supplementary material.

Acknowledgements

We would like to acknowledge Dr. Jim Babb, PhD for assistance with statistical analysis.

Funding

This work was supported by the department of radiology.

Conflict of interest

Two of the authors are employees of Siemens Healthcare/Healthineers. Under an existing research agreement, these authors provided technical support with the modification of the MRI system and with sequence modifications for operation at 0.55 T. These authors did not have control over any other aspect of the study design or the study results.

References

1. An JY, Pena MA, Cunha GM, et al. Abbreviated MRI for Hepatocellular Carcinoma Screening and Surveillance. Radiographics. 2020;40(7):1916–1931. [PubMed: 33136476]
2. Besa C, Lewis S, Pandharipande PV, et al. Hepatocellular carcinoma detection: diagnostic performance of a simulated abbreviated MRI protocol combining diffusion-weighted and T1-weighted imaging at the delayed phase post gadoxetic acid. Abdom Radiol (NY). 2017;42(1):179–190. [PubMed: 27448609]
3. Feng L, Benkert T, Block KT, Sodickson DK, Otazo R, Chandarana H. Compressed sensing for body MRI. J Magn Reson Imaging. 2017;45(4):966–987. [PubMed: 27981664]
4. Hammernik K, Klatzer T, Kobler E, et al. Learning a variational network for reconstruction of accelerated MRI data. Magn Reson Med. 2018;79(6):3055–3071. [PubMed: 29115689]
5. van Beek EJR, Kuhl C, Anzai Y, et al. Value of MRI in medicine: More than just another test? J Magn Reson Imaging. 2019;49(7):e14–e25. [PubMed: 30145852]
6. Runge VM, Heverhagen JT. Advocating the Development of Next-Generation, Advanced-Design Low-Field Magnetic Resonance Systems. Invest Radiol. 2020;55(12):747–753. [PubMed: 33156083]
7. Bhat SS, Fernandes TT, Poojar P, et al. Low-Field MRI of Stroke: Challenges and Opportunities. J Magn Reson Imaging. 2020:e27324.
8. Sheth KN, Mazurek MH, Yuen MM, et al. Assessment of Brain Injury Using Portable, Low-Field Magnetic Resonance Imaging at the Bedside of Critically Ill Patients. JAMA Neurol. 2020.
9. Algarin JM, Diaz-Caballero E, Borreguero J, et al. Simultaneous imaging of hard and soft biological tissues in a low-field dental MRI scanner. Sci Rep. 2020;10(1):21470. [PubMed: 33293593]
10. Campbell-Washburn AE, Ramasawmy R, Restivo MC, et al. Opportunities in Interventional and Diagnostic Imaging by Using High-Performance Low-Field-Strength MRI. Radiology. 2019;293(2):384–393. [PubMed: 31573398]

11. Heiss R, Grodzki DM, Horger W, Uder M, Nagel AM, Bickelhaupt S. High-performance low field MRI enables visualization of persistent pulmonary damage after COVID-19. Magn Reson Imaging. 2021;76:49–51. [PubMed: 33220447]
12. Bandettini WP, Shanbhag SM, Mancini C, et al. A comparison of cine CMR imaging at 0.55 T and 1.5 T. J Cardiovasc Magn Reson. 2020;22(1):37. [PubMed: 32423456]
13. Pipe JG. Motion correction with PROPELLER MRI: application to head motion and free-breathing cardiac imaging. Magn Reson Med. 1999;42(5):963–969. [PubMed: 10542356]
14. Pfeuffer J, van de Moortele PF, Yacoub E, et al. Zoomed functional imaging in the human brain at 7 Tesla with simultaneous high spatial and high temporal resolution. Neuroimage. 2002;17(1):272–286. [PubMed: 12482083]
15. Eggers H, Brendel B, Duijndam A, Herigault G. Dual-echo Dixon imaging with flexible choice of echo times. Magn Reson Med. 2011;65(1):96–107. [PubMed: 20860006]
16. Knoll F, Murrell T, Sriram A, et al. Advancing machine learning for MR image reconstruction with an open competition: Overview of the 2019 fastMRI challenge. Magn Reson Med. 2020;84(6):3054–3070. [PubMed: 32506658]

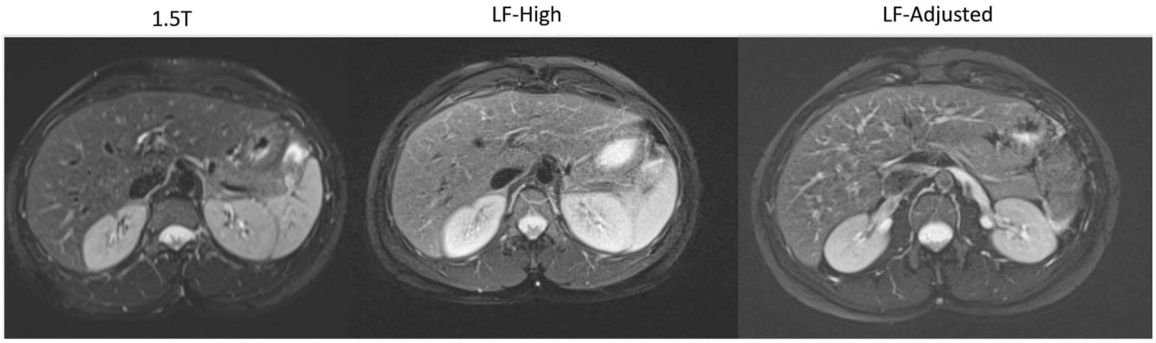

Fig. 1.

Representative axial T2WI slice in the same volunteer imaged in 1.5 T, LF-High, and LF-Adjusted scanner configurations

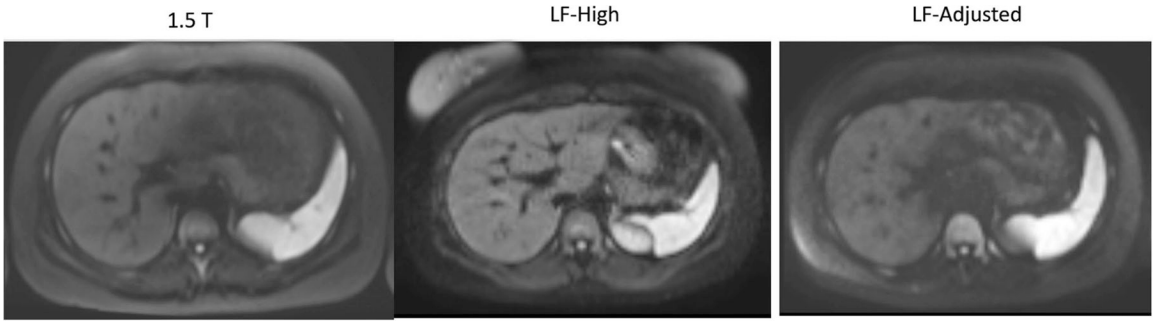

Fig. 2.

Representative axial high *b*-value image from DW acquisition in the same volunteer imaged in 1.5 T, LF-High, and LF-Adjusted scanner configurations

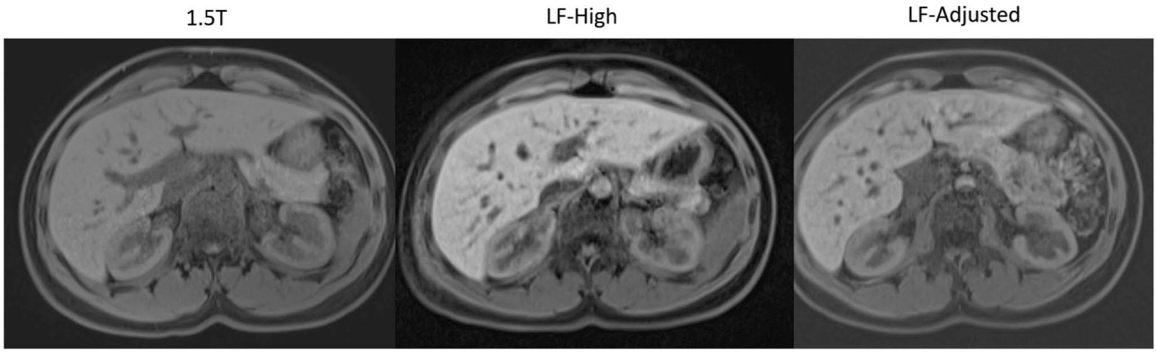

Fig. 3.

Representative axial T1FS (water only) image from Dixon T1W acquisition in the same volunteer imaged on 1.5 T, LF-High, and LF-Adjusted scanner configurations

Abdom Radiol (NY). Author manuscript; available in PMC 2022 January 02.

Table 1

Acquisition parameters of the optimized sequences for (A) 0.55 T with higher-performance gradients (“High Gradient”), (B) 0.55 T with lower-performance adjusted gradients (“Lower Adjusted Gradient”), and (C) 1.5 T with conventional gradients for comparison

0.55 T high gradient	**T2 fat sat**	**DWI**	**DIXON VIBE**
Flip angle (deg)	180	90	25
TR/TE (ms)	4000/68	4900/55	8.83
			TE1 2.56
			TE2 = 6
Readout bandwidth (Hz/Px)	306	1220	480
Slice thickness (mm)	6	6	6 (Interpolated to 3 mm)
Number of slices	32	32	72
FOV (cm)	38 × 38	38 × 28.5	38 × 30
Resolution (mm^2)	1.2 × 1.2	3 × 3	1.3 × 1.3
Acceleration type	GRAPPA	GRAPPA	CAIPIRINHA
Acceleration factor	2	2	4 (2 × 2)
Partial Fourier	–	6/8	PE = 6/8
			Slice = 6/8
Averages	1	B value 50 = 2	1
		B value 500 = 4	
		B value 800 = 14	
Acquisition time	3 min 14 s	5 min 9 s	16 s
0.55 T lower adjusted gradient	**T2 fat sat**	**DWI**	**DIXON VIBE**
Flip angle (deg)	180	90	25
TR/TE (ms)	4000/80	4900/75	8.83
			TE1 = 2.56
			TE2 = 6
Readout bandwidth (Hz/Px)	306	1220	480
Slice thickness (mm)	6	6	6 (Interpolated to 3 mm)
Number of slices	32	32	72
FOV (cm)	38 × 38	38 × 28.5	38 × 30
Resolution (mm^2)	1.2 × 1.2	3 × 3	1.3 × 1.3

0.55 T high gradient	**T2 fat sat**	**DWI**	**DIXON VIBE**
Acceleration type	GRAPPA	GRAPPA	CAIPIRINHA
Acceleration factor	2	2	4 (2 × 2)
Partial Fourier	–	6/8	PE = 6/8 Slice = 6/8
Averages	1	B value 50 = 2 B value 500 = 4 B value 800 = 14	1
Acquisition time	3 min 14 s	5 min 9 s	16 s
1.5 T conventional gradient	**T2 fat sat**	**DWI**	**DIXON VIBE**
Flip angle (deg)	170	90	10
TR/TE (ms)	3500/90	4900/55	6.8/2.39 TE2 = 4.77
Readout bandwidth (Hz/Px)	300	1148	600
Slice thickness (mm)	4	6	6 (Interpolated to 3 mm)
Number of Slices	44	30	72
FOV (cm)	35 × 35	38 × 26	38 × 30
Resolution (mm^2)	1.4 × 1.4	3 × 3	1.3 × 1.3
Acceleration type	GRAPPA	GRAPPA	CAIPIRINHA
Acceleration factor	2	2	4 (2 × 2)
Partial Fourier	–	6/8	PE = 6/8 Slice = 6/8
Averages	1	B value 50 = 2 B value 500 = 4 B value 800 = 14	1
Acquisition time	53 s	5 min 9 s	10 s

Table 2

Image quality parameters and scores for various imaging contrasts

Image quality parameter	Image contrast	Score
Overall image quality	T2W, DWI, T1FS, T1 in- and out-of-phase	1 = Non-diagnostic; 2 = poor; 3 = Acceptable; 4 = Good; 5 = excellent
Posterior right hepatic lobe sharpness	T2W, DWI, T1FS, T1 in- and out-of-phase	1 = Unacceptable (non-diagnostic); 2 = poor (extreme blur); 3 = fair (moderate blur); 4 = Good (mild blur); 5 = excellent (no blur)
Clarity of hepatic vessel	T2W, DWI, T1FS, T1 in- and out-of-phase	1 = Unacceptable (invisible MPV); 2 = poor (only MPV visible); 3 = fair (only main branch of portal vein visible); 4 = good (some peripheral portal veins visible); 5 = Excellent (peripheral portal veins clearly visible)
Conspicuity of the left lobe	DWI	1 = Unacceptable (non-diagnostic); 2 = poor (extreme blur); 3 = fair (moderate blur); 4 = Good (mild blur); 5 = excellent (no blur)

Abdom Radiol (NY). Author manuscript; available in PMC 2022 January 02.

Table 3

Overall image quality scores by type of image contrast and reader

T2WI	**Low-field High**	**Low-field Adjusted**	**1.5 T**
Reader 1	4.30 ± 0.82	3.90 ± 0.74	4.50 ± 0.71
Reader 2	3.60 ± 0.70	4.00 ± 0.67	4.70 ± 0.48
Reader 3	4.40 ± 0.70	4.40 ± 0.52	4.60 ± 0.52
Average	4.1 ± 0.6	4.1 ± 0.6	4.6 ± 0.4
DWI	**Low-field High**	**Low-field Adjusted**	**1.5 T**
Reader 1	3.80 ± 0.79	3.30 ± 0.95	4.70 ± 0.67
Reader 2	4.20 ± 0.42	4.40 ± 0.7	4.50 ± 0.53
Reader 3	4.40 ± 0.84	4.60 ± 0.52	4.50 ± 0.71
Average	4.13 ± 0.48	4.10 ± 0.57	4.57 ± 0.39
T1 In & Out	**Low-field High**	**Low-field Adjusted**	**1.5 T**
Reader 1	4.25 ± 0.46	4.10 ± 0.32	5.00 ± 0.0
Reader 2	4.63 ± 0.52	4.60 ± 0.52	4.80 ± 0.42
Reader 3	4.50 ± 0.53	4.60 ± 0.52	5.00 ± 0.0
Average	4.46 ± 0.40	4.43 ± 0.32	4.93 ± 0.14
T1FS	**Low-field High**	**Low-field Adjusted**	**1.5 T**
Reader 1	4.00 ± 0.47	4.00 ± 0.0	5.00 ± 0.0
Reader 2	4.60 ± 0.52	4.40 ± 0.52	4.90 ± 0.32
Reader 3	4.30 ± 0.48	4.40 ± 0.52	5.00 ± 0.0
Average	4.30 ± 0.29	4.27 ± 0.21	4.97 ± 0.11

Abdom Radiol (NY). Author manuscript; available in PMC 2022 January 02.

Table 4

Liver-to-muscle contrast ratio (Lc/Mc) for T2WI, DWI, and T1FS for LF-High, LF-Adjusted, and 1.5 T

L/M contrast ratio (Lc/Mc)	LF-high	LF-adjusted	1.5 T
T2WI	1.73 ± 0.26	1.89 ± 0.32	2.7 ± 0.44
DWI	2.30 ± 0.30	2.69 ± 0.53	1.45 ± 0.29
T1WI	1.92 ± 0.21	1.81 ± 0.25	1.46 ± 0.15